

Terahertz Response of a Microfabricated Rod–Split-Ring-Resonator Electromagnetic Metamaterial

H. O. Moser,* B. D. F. Casse, O. Wilhelmi, and B. T. Saw

Singapore Synchrotron Light Source, National University of Singapore, 5 Research Link, Singapore 117603, Republic of Singapore

(Received 15 December 2003; published 15 February 2005)

The first electromagnetic metamaterials (EM³) produced by microfabrication are reported. They are based on the rod–split-ring-resonator design as proposed by Pendry *et al.* [IEEE Trans. Microwave Theory Tech. **47**, 2075 (1999)] and experimentally confirmed by Smith *et al.* [Phys. Rev. Lett. **84**, 4184 (2000)] in the GHz frequency range. Numerical simulation and experimental results from far infrared (FIR) transmission spectroscopy support the conclusion that the microfabricated composite material is EM³ in the range 1–2.7 THz. This extends the frequency range in which EM³ are available by about 3 orders of magnitude well into the FIR, thereby widely opening up opportunities to verify the unusual physical implications on electromagnetic theory as well as to build novel electromagnetic and optical devices.

DOI: 10.1103/PhysRevLett.94.063901

PACS numbers: 42.70.Qs, 41.20.Jb, 73.20.Mf, 78.20.Ci

Introduction.—First theoretically analyzed by Veselago [1], electromagnetic metamaterials require both permittivity ϵ and permeability μ to be negative simultaneously. When this is the case, a wealth of unusual phenomena is predicted such as a left-handed coordinate frame to describe the electromagnetic fields and the wave vector, the Poynting and group velocity vectors pointing in a direction opposite to the wave vector, a negative index of refraction, and inverted Doppler and Čerenkov effects. Promising applications have been discussed [2], including the realization of a perfect lens [3].

There are no classical materials exhibiting simultaneously negative ϵ and μ . However, Pendry and co-workers analyzed schemes for obtaining $\epsilon_{\text{eff}} < 0$ [4] and $\mu_{\text{eff}} < 0$ [5] which feature arrays of thin wires and split-ring resonators. This concept was experimentally verified up to date in the microwave region [6], i.e., in the Gigahertz frequency range.

In the present work, microfabrication methods were used for the first time to reduce the overall structure size of rod–split-ring-resonators below 100 μm with structural details down to 5 μm , thus boosting the frequency at which the composite material exhibits electromagnetic metamaterial (EM³) behavior to a few THz. In terms of wavelength or wave numbers, this corresponds to 300 μm downwards and 33 cm^{-1} upwards, respectively, which is about 3 orders of magnitude higher than the hitherto known values in the microwave range. There is a further potential to reduce sizes to reach the near infrared spectral range at about 2 μm wavelength.

To produce the composite materials, we use lithography-based micro- and nanofabrication including the LIGA (Lithographie, Galvanoformung and Abformung) process [7]. These techniques do not only allow us to reduce dimensions to the μm and nm scales, but they also open up many possibilities such as arbitrary shapes of the structures, the use of a variety of materials, and the fabrication

of larger quantities for 3D stacking based on batch processing and hot embossing, all of them important in view of practical applications. The design data of the structures are determined using Pendry's analytical formulas as well as numerical simulation by means of Microwave Studio (MWS) [8], a state-of-the-art electromagnetic field solver, which is based on the finite integration technique with the perfect boundary condition approximation [9]. The spectral response of the material is measured using Fourier transform interferometry.

Simulation.—From Pendry's formulas for the split-ring structure μ_{eff} [5] we obtain the lower and upper bounds of the frequency interval over which $\mu_{\text{eff}} < 0$ as

$$\nu_0 = \frac{1}{2\pi} \sqrt{\frac{3dc_0^2}{\pi^2 r^3}} < \nu_{\text{mp}} = \frac{\nu_0}{\sqrt{1 - \pi r^2/ab}}, \quad (1)$$

where c_0 is the speed of light *in vacuo*. The ϵ of wire arrays can be kept negative over a wide range using a sufficiently small ratio of radius to distance. Figure 1 shows an overview of the structures and the parameters used to calculate them. Five geometric variants are considered here, involving four different radii and a fat version. The sets of geometric parameters and boundary frequencies for a

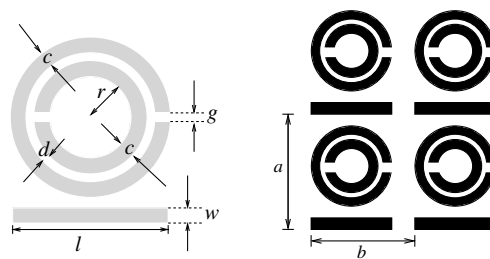


FIG. 1. Geometric parameter definition of the RSR (left). Periodic arrangement of the RSR adopted for microfabrication (right).

TABLE I. THz specifications of a rod-split-ring structure.^a

	$r/\mu\text{m}$	$c/\mu\text{m}$	$d/\mu\text{m}$	$a/\mu\text{m}$	$b/\mu\text{m}$	ν_0/THz	$\nu_{\text{mp}}/\text{THz}$
Ni slim	10	10	10	110	90	2.63	2.68
Ni fat	10	15	10	135	110	2.63	2.67
Au 1	8.4	12	4.3	95.4	78.4	2.24	2.28
Au 2	11	12	4.3	100.6	83.6	1.50	1.53
Au 3	14	12	4.3	106.6	89.6	1.04	1.08

^aFor all structures $g = 5 \mu\text{m}$, $l = (r + 2c + d) \times 2$. For Ni, $w = 10 \mu\text{m}$ while for Au, $w = 12 \mu\text{m}$.

rod-split-ring (RSR) patterned material to become left-handed in the lower THz spectral range are given in Table I. Numerical simulations of a plane wave impinging on the RSR composite structure were performed using the MWS code. Three angles of incidence were chosen, namely 0° , 45° , and 90° , with the magnetic field pointing along the split-ring axes in the latter case. The electric field was polarized either parallel or perpendicular to the rods. It was confirmed that the case of 90° incidence angle to the normal and the \mathbf{E} field parallel to the rods showed the signature of the metamaterial most clearly.

In Fig. 2 the ratio of the amplitudes of the transmitted and incident waves, respectively, S_{21} , as used in the MWS code, is shown for the individual cases of rods only, split-ring resonators (SRR), and RSR for the Ni slim ring. The transmission of either rods or SRRs is small, indicating negative ϵ_{eff} and μ_{eff} , respectively, while the composite material shows a transmission peak as expected.

Microfabrication.—In order to produce EM³ materials for transmission experiments according to the simulations above, split rings and rods have to be embedded in a material that features high transparency in the THz frequency range itself. Moreover, such composite EM³ materials need to be released from the substrate and must be sufficiently rugged to survive transmission experiments without damage.

AZ P4620 photoresist [10] was chosen because it was expected to exhibit very good transmission in the THz

frequency range, to allow RSR micropatterning by direct laser writing [11], and it appeared to have sufficient mechanical strength to be handled after release from the substrate. Four-inch silicon wafers were used as a substrate for the microfabrication process to ensure compatibility with all process equipment at Singapore Synchrotron Light Source (SSLS). First a sacrificial layer of 200 nm Cr was deposited by magnetron sputtering in order to facilitate the release of the EM³ material at the end of the microfabrication process. For the later electroplating of split rings and rods 15 nm Cu were deposited on top as the seed layer. The AZ P4620 photoresist was spin coated onto the wafer such that a thickness of 14 μm was achieved after the soft bake. For rapid prototyping, design files with split rings and rods with the parameters specified in Table I were generated in $2 \times 2 \text{ mm}^2$ arrays and transferred into the AZ P4620 photoresist using direct laser writing with the DWL 66 [12]. The DWL 66 is equipped with a 20 mW HeCd laser of 442 nm wavelength. The 20 mm write head employed for this experiment allows minimum feature dimensions of 4 μm . A double pass exposure is employed as this was found to yield better structure quality. After the direct laser writing the resist is developed in the AZ 400K developer, rinsed with deionized water, and subsequently hard baked. A gentle oxygen plasma etch is applied to remove residual resist in the developed areas.

The wafer with the photoresist template is brought into a Ni (Ni slim and fat rings) or Au (Au sample 1,2 and 3) electroplating bath in order to realize Ni or Au split rings and rods. Electroplating is carried out at a current density of 1 A/dm² for Ni and 0.1 A/dm² for Au at a temperature of 55 °C. Care is taken to avoid overplating. Figure 3

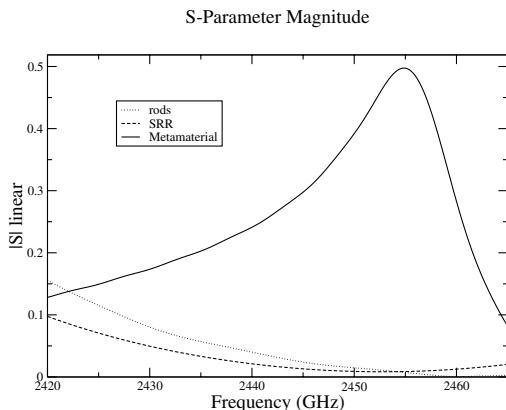


FIG. 2. Amplitude ratio of transmitted and incident waves as expressed by the parameters S_{21} (linear scale) in MWS for the rods, SRR and RSR.

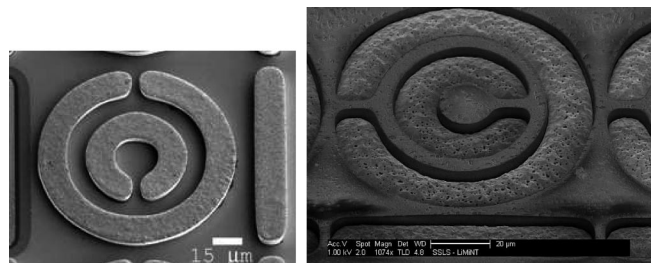


FIG. 3. Electroplated RSR structures of nickel with resist stripped off (left, scale bar 15 μm) and gold embedded in resist AZP4620 (right, scale bar 20 μm).

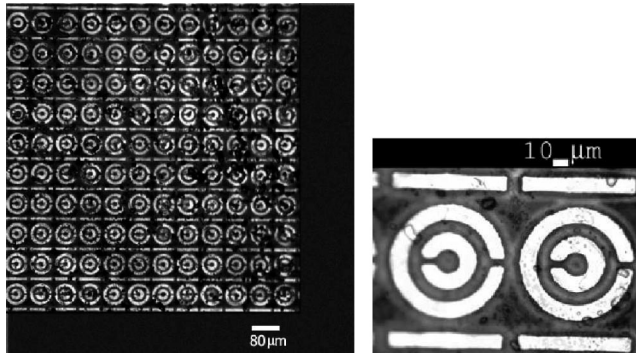


FIG. 4. A bird's eye view (left) and a close-up (right) of 2.1 mm × 2.1 mm microchips of Ni metamaterial embedded in a plastic (AZ P4620) matrix.

shows RSR after Ni or Au electroplating. The resist was removed in the case of nickel to investigate the structures in detail.

A final crucial step is to dice the structures and to free the composite material slabs from the substrate. Chips are cut out with a precision saw upon which the Cr sacrificial layer is removed using a Cr etch consisting of two parts deionized water and one part concentrated HCl. The final products are thin slabs consisting of Ni or Au RSRs held in a plastic matrix of AZ P4620 resist. The dimensions are 2.1 mm wide by 2.1 mm long by 14 μm thick as shown in Fig. 4.

Spectroscopic results.—The evidence that the composite materials presented here are left-handed is based on the demonstration that the frequency dependence follows the prediction by both Pendry's formulas and the numerical simulation when the geometric parameters are changed. Spectroscopic measurements were performed using a Bruker IFS 66 v/S Fourier transform interferometer (FTIR) in the far infrared over the range of 22 to 400 cm⁻¹ with 4 and 2 cm⁻¹ spectral resolution. The chips were mounted in the FTIR at normal incidence to the beam. Axial magnetic field components needed to induce the current in the split rings are due to misalignment of the sample with respect to the beam and diffraction at the

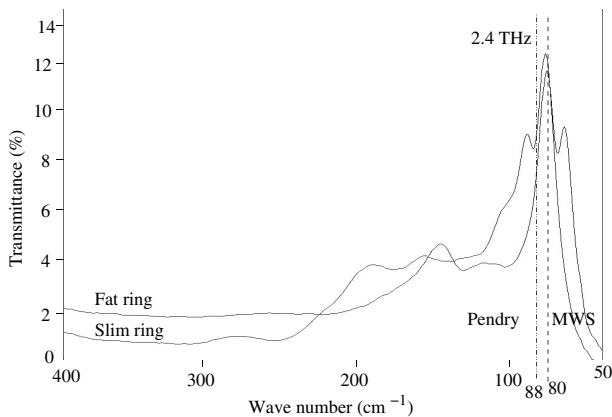


FIG. 5. Measured spectral response of the two Ni RSR.

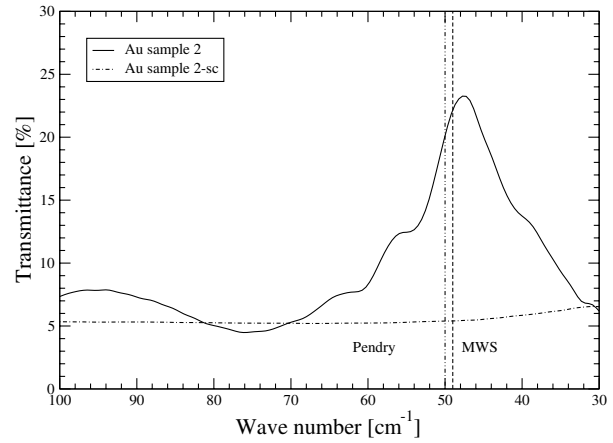


FIG. 6. Measured spectral response of an Au RSR structure (Au sample 2, solid line) and its short-circuited version (dash-dotted line). The vertical lines indicate the wave numbers of the maximum as predicted by the numerical simulation (MWS) and the analytical formulas (Pendry).

surface. The beam was unpolarized. Figures 5 and 6 display the response of the slim and fat Ni RSRs as well as the Au RSR sample 2 and its short-circuited version, respectively. The wave numbers at which the maxima occur agree reasonably with the values expected from the MWS simulation and the analytical Pendry formulas.

Figure 7 shows the position of the maxima for all cases versus the inner radius r . Measured and numerically simulated values are always quite close while the analytical formulas lead to an up to 17% deviation in the case of Au sample 3.

The three Au cases show a good $r^{-3/2}$ dependence as all other parameters were kept constant. In the Ni case, the frequency is higher as the annular gap between the inner and outer rings, d , is larger by more than a factor of 2, thus

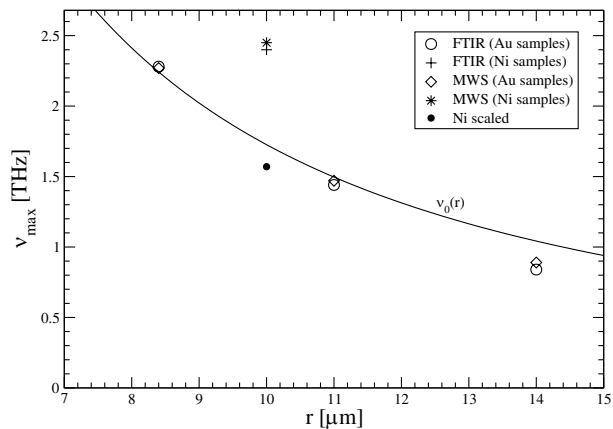


FIG. 7. Frequencies of the maxima of the spectral response curves versus the inner radius of the split-ring resonators for the measured (FTIR) and numerically simulated (MWS). The solid curve shows $\nu_0(r)$ of Eq. (1) for the Au cases. When the Ni case is scaled to the same d as for Au it also comes close to the curve (●).

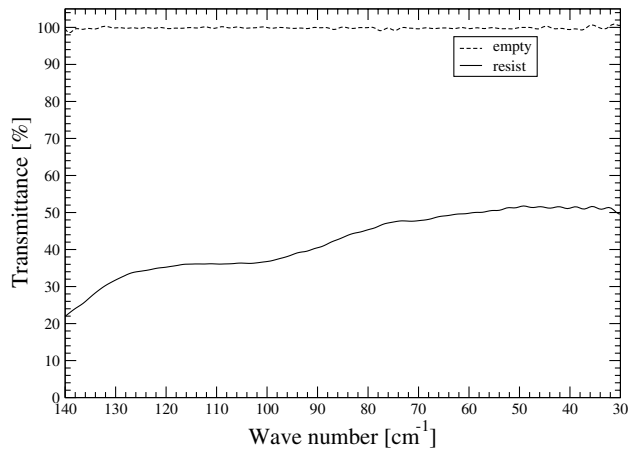


FIG. 8. Spectrum with a resist slab only and without any sample.

reducing capacitance and increasing resonance frequency. However, when it is scaled to the same value of d as for Au it also comes close to the curve. As further evidence, one of each sample was fabricated with the gap g of the split rings closed, thus removing a decisive structure element of the split-ring resonator. As expected, the closed ring structure does not show any resonant behavior in the relevant frequency range (Fig. 6).

Figure 8 shows the transmission without any sample and with the resist slab only to be more or less flat as compared to the peaks.

Conclusion.—Composite materials consisting of an array of Ni or Au split-ring resonators and rods embedded in an AZ P4620 resist matrix were produced using lithography-based micro- or nanofabrication. With an outer ring diameter of 73.4–100 μm , analytical and numerical simulations predict the spectral resonance of the structures to occur between 1 and 2.7 THz. Spectral measurements with a Fourier transform interferometer performed for various RSR arrays with different geometric parameters show the transmission peaks in the far infrared at wave numbers corresponding closely to the prediction.

This is evidence for the conclusion that these composite materials exhibit EM³ properties in the 1–2.7 THz spectral range. Thus, the present work extends, by about 3 orders of magnitude, the spectral range accessible for experimentally verifying the many unusual physical implications of

EM³ on electromagnetic theory and for building novel electromagnetic and optical devices.

From the micro- or nanofabrication point of view there is a further potential to reduce sizes to reach the near infrared spectral range at about a 2 μm wavelength.

The authors thank Professor Lim Hock, Dr. Sergei Matitsine, and Gan Yeow Beng of the Temasek Laboratories, National University of Singapore, for stimulating discussions. They also thank Bruker Optics for providing fast access to one of their FTIR for the Ni RSR measurements and acknowledge the contribution of the SSLS LiMiNT staff, J.R. Kong and Shahrain bin Mahmood, for developing and optimizing microtechnology processes. The work was performed at SSLS under A*STAR/MOE RP3979908M and NUS Core Support C-380-003-003-001 grants.

*To whom all correspondence should be addressed.

Electronic address: moser@nus.edu.sg

- [1] V. G. Veselago, *Usp. Fiz. Nauk* **92**, 517 (1964) [*Sov. Phys. Usp.* **10**, 509 (1968)].
- [2] N. Engheta, in *Advances in Electromagnetics of Complex Media and Metamaterials* (Kluwer Academic, Dordrecht, London, 2003).
- [3] J. B. Pendry, *Phys. Rev. Lett.* **85**, 3966 (2000).
- [4] J. B. Pendry, A. J. Holden, W. J. Stewart, and I. Youngs, *Phys. Rev. Lett.* **76**, 4773 (1996).
- [5] J. B. Pendry, A. J. Holden, D. J. Robbins, and W. J. Stewart, *IEEE Trans. Microwave Theory Tech.* **47**, 2075 (1999).
- [6] D. R. Smith, W. J. Padilla, D. C. Vier, S. C. Nemat-Nasser, and S. Schultz, *Phys. Rev. Lett.* **84**, 4184 (2000).
- [7] E. W. Becker, W. Ehrfeld, P. Hagmann, A. Maner, and D. Muenchmeyer, *Microelectron. Eng.* **4**, 35 (1986).
- [8] Microwave Studio is a registered trademark of CST GmbH, Darmstadt, Germany.
- [9] T. Weiland, R. Schuhmann, R. B. Gregor, C. Parazzoli, and A. M. Vetter, *J. Appl. Phys.* **90**, 5419 (2001).
- [10] AZP4620 is a registered trademark of Clariant Corporation, Business Unit Electronic Materials, New Jersey, USA.
- [11] Y. Cheng, T. Huang, and C. C. Chieng, *Microsys. Tech.* **9**, 17 (2002).
- [12] DWL 66 is a registered trademark of Heidelberg Instruments Mikrotechnik GmbH, Germany.